Energy radiation and limiting speeds of fast moving edge dislocations in tungsten

Zhaohui Jin*
Institut für Zuverlässigkeit von Bauteilen und Systemen (IZBS), Universität Karlsruhe (TH), Kaiserstrasse 12, 76131 Karlsruhe, Germany and School of Materials Science and Engineering, Shanghai Jiao Tong University, Shanghai 200240, People's Republic of China

Huajian Gao
Division of Engineering, Brown University, Providence, Rhode Island 02912, USA

Peter Gumbsch
Institut für Zuverlässigkeit von Bauteilen und Systemen (IZBS), Universität Karlsruhe (TH), Kaiserstrasse 12, 76131 Karlsruhe, Germany and Fraunhofer Institut Werkstoffmechanik (IWM), Wöhlerstrasse 11, 79108 Freiburg, Germany

(Received 6 November 2007; revised manuscript received 11 January 2008; published 11 March 2008)

The energy loss of a uniformly moving dislocation radiating lattice waves is quantitatively studied by atomistic simulations. The velocity dependence of the energy radiation provides a unique way to understand limiting behavior exhibited by fast moving dislocations. In combination with theoretical analyses, the simulations provide a consistent atomic-level picture of near-sonic, transonic, and supersonic dislocation motions in crystalline materials.

DOI: 10.1103/PhysRevB.77.094303 PACS number(s): 61.72.Lk, 62.30.+d, 47.40.Hg, 46.70.Lk

I. INTRODUCTION

Plastic deformation of a crystalline material relies on the motion of dislocations, line defects of the crystal lattice. Dislocations release elastically stored strain energy as they move. The rate of deformation is given by the product of dislocation density and mobility.[1] Mobile dislocations may achieve high speeds at high levels of stress or strain, close to or even exceeding sound velocities in the elastic media.[2–5] In spite of its fundamental and practical importance, many aspects on the physical nature of fast moving dislocations remain uncertain.

The motion of dislocations can be limited by many factors, such as the existence of impurities, interstitials, vacancies, grain boundaries, and other dislocations. Even under ideal circumstances, the behavior of a moving dislocation is limited by phonon-related damping forces due to lattice waves both radiated from and scattered around the dislocation.[6–11] For fast moving dislocations at and above the shear wave speed, it has long been realized and also demonstrated in recent molecular dynamics (MD) simulations[5] that radiation damping plays an essential role.

According to linear elasticity theory,[2–4] dislocations can move faster than both transverse and longitudinal elastic waves (lattice phonons in the long wavelength limit) which propagate at the sound wave speeds c_t and c_l, respectively. The theoretical predictions have inspired a number of recent efforts to observe and understand limiting behavior of transonic and supersonic dislocations in computer experiments.[5,12–21] Somewhat related physical phenomena, however, have been observed in both simulations and experiments for different subjects such as propagating shear cracks,[22–25] mechanical twinning,[26–28] phase transition due to shock waves,[29] dust particle motion in plasmas,[30] as well as ruptures and earthquakes.[31,32] Although direct experimental evidence appears rare for metals, the nucleation of transonic and/or supersonic dislocations in plasmas crystals has been observed recently.[33]

In contrast to continuum mechanical assumptions that dislocations in fast and uniform motion can be studied with reference to "radiation-free" states both below and above c_t, true lattice dislocations always generate lattice waves and thus radiate energy. Except for Koizumi and coworkers,[14,15] little attention has been paid to clarify the force-velocity relation associated with the energy radiation of fast moving dislocations in discrete and periodic lattices.

To identify the limiting speeds and to measure exactly the radiation damping are critical to understand the motion of dislocations at high velocities. For this purpose, we performed a systematic study of straight and uniformly moving edge dislocations by MD simulations presented here.

II. METHODS

A straight edge dislocation within a three-dimensional block of a body-centered cubic (bcc) lattice is considered in our simulations (Fig. 1). The Burgers vector of the perfect dislocation is aligned along the x direction and is given by $\mathbf{b}=\frac{a_0}{2}[\bar{1}1\bar{1}]$, where a_0 is the lattice parameter (3.165 Å for W at 0 K). The direction of dislocation line is [110] which is the z direction pointing out of the paper in Fig. 1. Periodic boundary conditions are imposed in both x and z directions such that the dislocation remains straight at the central glide plane. In the third direction (y), the dislocated crystal is confined by two rigid borders. The volume of the MD slab is $V=l_x\times 2l_y\times l_z\approx 131.75\sqrt{3}a_0\times 52\sqrt{6}a_0\times 4\sqrt{2}a_0$ and contains 322 523 atoms which are allowed to move freely. The dislocated crystal is fully relaxed and the kinetic energy of the system is zero prior to loading. The motion of the dislocation is then studied by instantaneously applying a homogeneous simple shear (ε_{appl}) to the entire system, defined according to

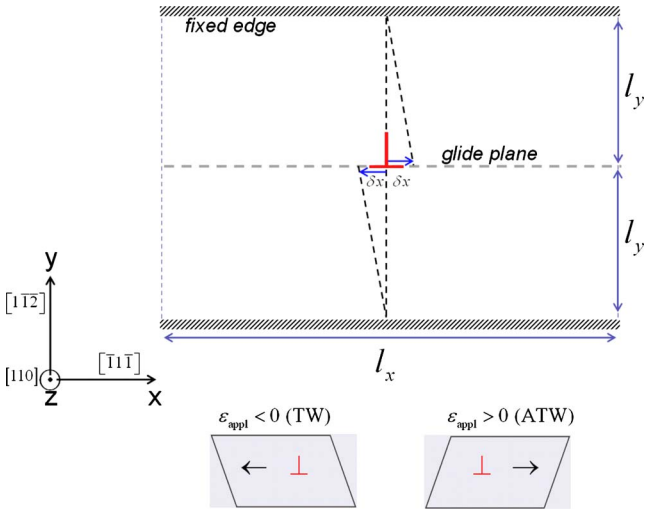

FIG. 1. (Color online) Schematic drawing of a perfect edge dislocation $\left(\mathbf{b}=\frac{1}{2}[\bar{1}1\bar{1}]\right)$, located in the center of the simulation box. The dislocation may glide either to the twinning (TW) or to the antitwinning (ATW) direction, depending on the direction of applied shear.

$\varepsilon=(\partial/\partial y)u_x$, where u_x is the displacement in the x direction.

Within the confined slab of lattice, the strain released by the dislocation with Burgers vector b moving a distance δx is given by $\delta\varepsilon=b\delta x/(2l_xl_y)$ according to the amount of relative slip below and above the glide plane. The change in elastic strain energy when the dislocation has moved by δx is given by $\delta W=\frac{1}{2}V\mu\varepsilon'^2-\frac{1}{2}V\mu\varepsilon^2$, where $\varepsilon'=\varepsilon_{appl}-\delta\varepsilon$, $\varepsilon\equiv\varepsilon_{appl}$, and μ is the shear modulus. It is easy to show that $\delta W/l_z\delta x=-\mu\varepsilon_{appl}b+O(\delta x)$. The driving force acting on the dislocation measures the work done (per unit length per unit distance of motion) by the shear stain and/or stress applied externally, which is

$$G_e=\lim_{\delta x\to 0}\frac{-\delta W}{l_z\delta x}=\mu\varepsilon_{appl}b. \tag{1}$$

This is the well-known Peach-Koehler driving force acting on a dislocation.[1]

The bcc metal tungsten (W) is considered here because it is almost isotropic. Its isotropy greatly simplifies comparison to elasticity theory significantly. The Finnis-Sinclair (FS) many-body potential[34,35] is used in our simulations to determine interatomic forces. For elastic analysis, the FS potential is assumed to remain isotropic even under large shear strains. Sound velocities are determined by $c_t=(c_{xyxy}/\rho)^{1/2}$ and $c_l=(c_{xxxx}/\rho)^{1/2}$, where c_{xyxy} and c_{xxxx} are the elastic constants relevant to our MD geometry and ρ is the density of the material. At $\varepsilon_{appl}=0$, c_{xxxx} and c_{xyxy} can be determined exactly using elastic constants C_{11}, C_{12}, and C_{66} for the cubic lattice according to $c_{xxxx}=\frac{1}{3}(C_{11}+2C_{12}+4C_{66})$ and $c_{xyxy}=\frac{1}{3}(C_{11}-C_{12}+C_{66})$.

The dislocation can move either to the right or to the left along the glide plane in Fig. 1 depending on the sign of the applied shear. Due to lattice asymmetry, the two directions of motion are different and they are usually referred to as the twinning (TW) direction for the dislocation moving to the left and the antitwinning (ATW) direction for moving to the right, as indicated in Fig 1. The driving force on the dislocation given by Eq. (1) is a function not only of ε_{appl} but also of the shear modulus μ which in turn is a function of strain. To include nonlinear effects, the dependence of the elastic moduli on the applied strain ε_{appl} has been studied separately according to the shear response of a perfect lattice with the same geometry as the dislocated crystal (Fig. 1). The shear modulus is determined to be $\mu=c_{xyxy}\simeq 159.51-402.46\varepsilon_{appl}+1244.8\varepsilon_{appl}^2$ (in gigapascals) for $0\leqslant\varepsilon_{appl}\leqslant 11.5\%$ in the ATW direction and $159.51-480.66\varepsilon_{appl}+1325.4\varepsilon_{appl}^2$ (in gigapascals) for $-5.5\%\leqslant\varepsilon_{appl}\leqslant 0$ in the TW direction. The lattice itself is unable to sustain a rigid shear beyond the range $-5.5\%\leqslant\varepsilon_{appl}\leqslant 11.5\%$. The low values of the theoretical strength of the crystal, measured by a critical strain, 5.5% (or a critical stress, 10.0 GPa) in the TW direction and 11.5% (or 14.5 GPa) in the ATW direction, is a particular property of the FS model. The large difference in the TW and ATW directions, however, are expected from lattice symmetry.[36,37]

MD simulations are carried out in the *NVE* ensemble with a time step of 2 fs. The motion of dislocations is always adiabatic. Similar to previous studies,[5] the steady-state motion has been monitored to measure the dislocation velocity (v) versus the applied shear strain (ε_{appl}). The time window for the observation of steady-state motion depends on system size. As a constant ε_{appl} is applied instantaneously at $t=0$, the dislocation initially experiences a transient acceleration. After typically a few picoseconds, it reaches a constant velocity which we identify as the "steady state." If the simulation is allowed to run continuously without limiting the observation time, lattice waves reflected by the borders of the system interact with the dislocation and the effective driving force decreases as the dislocation runs out and in the MD box along the glide plane due to the periodic boundary conditions. The slab size in our simulations is chosen to be large enough such that a time window of about 10 ps is typically available for the observation of the steady-state motion under a homogeneous shear. Dislocation velocity is measured by locating the dislocation core in regular time intervals.

At small driving forces, $\varepsilon_{appl}<0.5\%$, the dislocation motion appears to be unsteady during the time of our simulations and no really well-defined uniform motion is observable. An average velocity is quoted in this regime, while steady-state velocities are quoted otherwise.[38] Damping due to the scattering of lattice phonons (temperature effects) is examined separately by introducing a finite temperature to the dislocated crystal with sufficient thermal equilibration prior to loading.

III. LIMITING SPEEDS

Dislocation motion has been monitored by measuring the velocity (v) of the dislocation versus the applied shear strain (ε_{appl}), as shown in Fig. 2. Three distinct velocity regimes can be identified: subsonic motion ($v<c_t$ at $-0.04<\varepsilon_{appl}\leqslant 0.065$), transonic motion in the antitwinning direction ($\sqrt{2}c_t<v<c_l$ at $0.025<\varepsilon_{appl}<0.07$), and supersonic motion

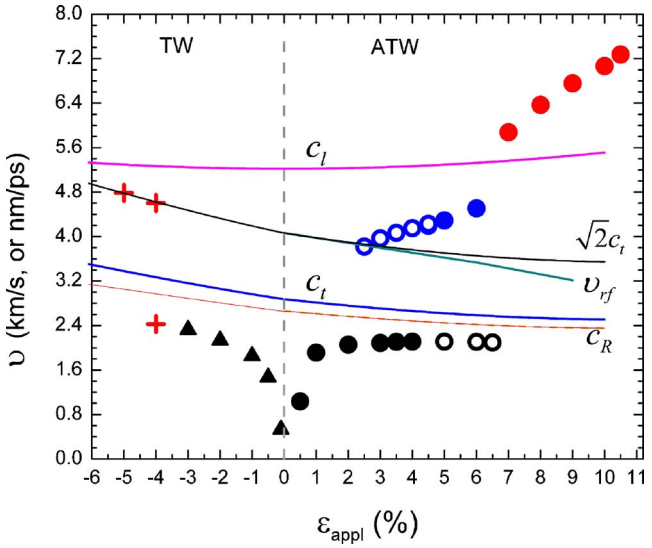

FIG. 2. (Color online) Dislocation velocity as a function of applied strain for uniform dislocation motion, obtained by MD simulations. Full symbols represent velocities achieved by applying a constant shear strain to a standstill dislocation (with zero initial temperature); open ones correspond to velocities reached by gradually changing the strain to a higher or lower value after uniform motion in a certain velocity regime has been established.

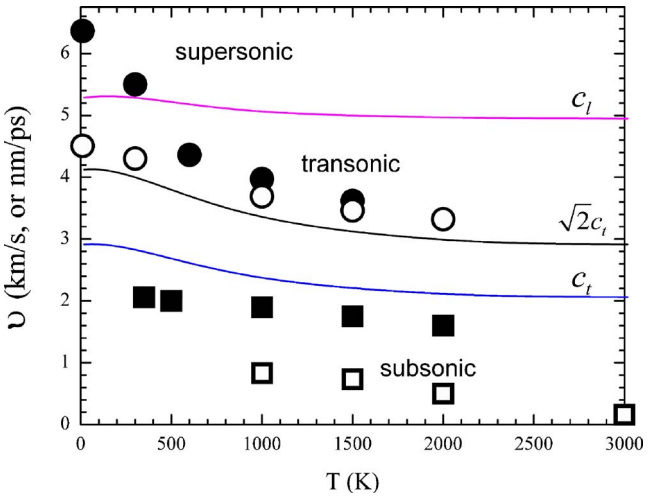

FIG. 3. (Color online) The velocity of uniform dislocation motion at finite temperature (T) for $\varepsilon_{appl}=4\%$ (filled squares), $\varepsilon_{appl}=6\%$ (open circles), and $\varepsilon_{appl}=8\%$ (filled circles). Sound wave speeds were calculated according to the T dependence of the corresponding Born moduli of the bulk lattice, obtained via MD simulations at thermal equilibrium.

($v > c_l$ at $0.07 \leqslant \varepsilon_{appl} < 0.11$). In the twinning direction, transonic motion is not observed for perfect dislocations but only for twinning. No stable dislocation motion is found in the velocity regime ($c_t < v < \sqrt{2}c_t$), in accordance with solutions of linear elasticity theory.[4] These results agree with previous MD observations[5] using a somewhat different method to insert dislocations into the system.

At subsonic velocities, a monotonic increase of v with ε_{appl} can be observed up to $\varepsilon_{appl} \sim 1\%$, followed by a regime of almost constant velocity, ~ 2100 m s^{-1}, with further loading up to $\varepsilon_{appl} \sim 7\%$. The constant velocity corresponds to a slight increase of v/c_t if the dependence of c_t on ε_{appl} (nonlinear effects) is considered. All subsonic motion is below the Rayleigh wave speed $c_R \sim 0.93 c_t$ (Ref. 4). The minimum velocity at which transonic motion is found stable is 3860 ± 100 m s^{-1} at $\varepsilon_{appl}=2.5\%$, very close to $\sqrt{2}c_t$. It appears that the so-called "radiation-free state" at $v_{rf}=\sqrt{2}c_t$ from linear elasticity analyses[4,5] sets the lower limit of transonic motion in a strictly isotropic elastic solid. Supersonic motion can be reached at $\varepsilon_{appl} > 6.5\%$. A gap exists between transonic and supersonic motions.

If the dislocation moves in the twinning direction ("triangles" in Fig. 2), stable dislocation motion can only be observed in the subsonic regime for a strain up to $\varepsilon_{appl}=4\%$ beyond which the dislocation dissociates and the process leads to twin emission. Twinning partials can then also propagate at transonic velocities ("plus" in Fig. 2) in accordance with continuum theory.[24]

Since nonlinear effects turned out to be significant, one has to check if anisotropy effects are relevant. This has been done numerically with Barnett and Zimmerman's solutions[39] based on a Stroh anisotropic elasticity analysis. In general, these solutions predict three limiting sound velocities, c_3, c_2, and c_1 for anisotropic materials. We found $c_3 \simeq c_2 \simeq c_t$ and $c_1 \simeq c_l$ hold within 2% for FS W, given that $0 \leqslant \varepsilon_{appl} < 11.5\%$. This indicates that anisotropic effects should not play a significant role for transonic and supersonic dislocations in FS W.

In order to address the question whether the transonic and/or supersonic motion of individual dislocations is still possible in systems at finite temperatures, or whether it is hampered by phonon scattering, we therefore repeated our simulations at strains of 4%, 6%, and 8% with different initial temperatures of the sample. The resulting dislocation velocities are displayed in Fig. 3. We found that the limiting speeds remain but increasingly higher driving forces are required to sustain supersonic motion at higher temperatures up to 2000 K (the melting point of FS W is about 3700 K). However, at sufficiently high driving force, such as $\varepsilon_{appl}=6\%$, the transonic motion ($v > \sqrt{2}c_T$) is clearly stable throughout the entire range of temperatures examined.

IV. RADIATION FIELD, FLOW FIELD, AND TWINNING

To reveal dislocation dynamics in detail, both the radiation field and the flow field (the velocity field) are shown in Fig. 4 by MD snapshots for dislocations moving at different velocities (in the ATW direction). It is clearly seen that lattice dislocations radiate at all velocities. The amount of radiated energy is carried away by lattice waves which are emitted very differently for the different velocity regimes. Flow-field plots help us to identify that the emitted elastic waves contain both transverse and longitudinal components. The two types of waves, i.e., shear and compressive, are emitted together but decouple as they propagate. If moving faster than sound wave velocities, dislocations exhibit characteristic Mach lines, i.e., wave fronts of shear or longitudinal waves. In particular, the transonic dislocation is signified

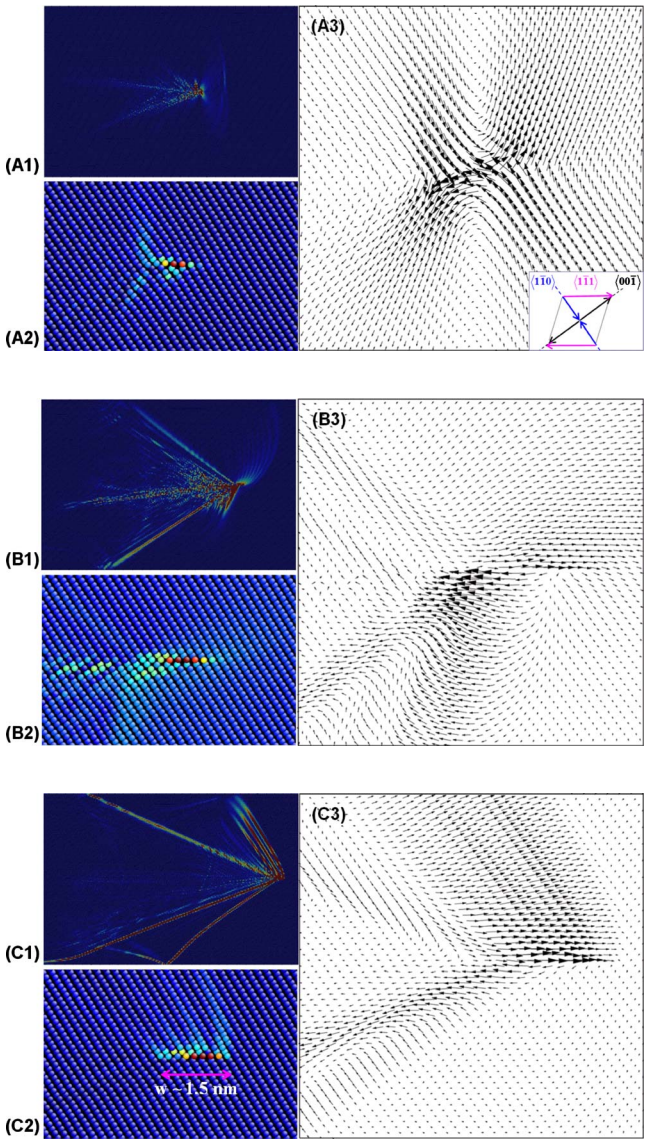

FIG. 4. (Color online) Atomic profiles of fast moving dislocations. (A) Subsonic motion: v=2.09 km s^{-1} at ε_{appl}=3%. (B) Transonic motion: v=4.51 km s^{-1} at ε_{appl}=6%. (C) Supersonic motion: v=6.76 km s^{-1} at ε_{appl}=9%. (i) Far-field snapshots of dislocation radiation (A1, B1, and C1), colored according to the transient "temperature" (kinetic energy) of individual atoms. (ii) Close view on core structures (A2, B2, and C2), colored according to the potential energy of individual atoms. (iii) Flow fields at dislocation core (A3, B3, and C3), measured by atomic displacements in the x-y plane ($\Delta\mathbf{u}$) within a time interval δt according to $\Delta\mathbf{u}(\delta t)=\Delta u_x(\delta t)\mathbf{i}+\Delta u_y(\delta t)\mathbf{j}$, where $\delta t=wv^{-1}$ with $w\approx 1.5$ nm (or $5\sim 6b$, which is of the order of the core width). Flow currents are dipolelike in orthogonal orientations as inset indicated (A3). For a better view of those localized shear wave fronts, Δu has been multiplied by a factor of 5 in these plots.

by a pair of shear wave Mach lines (Fig. 4, B1) and the supersonic dislocation is signified by Mach lines of both shear and compressive waves (Fig. 4, C1).

Subsonic dislocations moving into the TW direction at $\varepsilon_{appl}<4\%$ exhibit similar features, as shown by Fig. 4(a). Under larger applied strains, the dislocation dissociates according to $\mathbf{b}\rightarrow\mathbf{b}_t+\mathbf{b}_s$ [see Fig. 5(a)], where $\mathbf{b}_t=\frac{1}{6}[\bar{1}1\bar{1}]$ (a twinning partial) $\mathbf{b}_s=\frac{1}{3}[\bar{1}1\bar{1}]$ (a "sessile" partial), and the process triggers twin emission. Preceded by an individual emissary partial dislocation (Fig. 5, A and B), an advancing twin lamella with incoherent boundary may be generated by spontaneously nucleating dipolar twinning partial dislocations ($\frac{1}{6}[1\bar{1}1]$ and $\frac{1}{6}[\bar{1}1\bar{1}]$) on the fault plane between the original partials. The two twinning partials then move into opposite directions on the $(1\bar{1}2)$ glide plane parallel to the habit plane of the twin [Fig. 5(c)]. The observation supports the twinning mechanism proposed by Sleeswyk.[40] The number of twinning partials emitted determines the thickness of the twin under growth (typically, $\sim 10^2$ m s^{-1}). Measuring the velocity of twinning partials in our simulations, it is found that the forward twinning occurs at a transonic velocity and the backward twinning at a subsonic velocity [Fig. 5(d)].

V. ENERGY RADIATION ANALYSIS

To understand the forces governing dislocation motion, the energy release rate has been calculated to quantify the damping force due to radiation. In the following, we focus on the energy radiation analyses for uniformly moving dislocations in the ATW direction. However, the same analysis would also apply to the TW direction.

The total kinetic energy of the entire MD system of N atoms is calculated at any moment t according to

$$E_K(t)=\sum_{\alpha=1}^{N}\left[\frac{1}{2}m_\alpha\sum_{i=1}^{3}v_{i\alpha}^2(t)\right], \tag{2}$$

where $v_{i\alpha}$ is the ith component of the velocity vector of the αth atom. The kinetic energy can be rescaled in terms of an effective temperature for a NVE ensemble,

$$T_K(t)=E_K(t)/\left(\tfrac{3}{2}N-1\right)k_B, \tag{3}$$

which appears to be a linear function with simulation time for our simulations started at 0 K [Fig. 6(a)]. This indicates that a dislocation moving at a constant velocity v also radiates energy at a constant rate. Accordingly, the v dependence of energy radiation (G_K) or the kinetic energy released by a dislocation moving over a unit area (unit length of the dislocation times unit distance of motion) can be calculated explicitly by

$$G_K=\zeta^{-1}v^{-1}\frac{\delta E_K}{\delta t}, \tag{4}$$

where $v\delta t$ is the distance of motion within a time interval δt and ζ is the total length of dislocation in our MD box, $\zeta\equiv l_z$. Since both v and $\delta E_K/\delta t$ can be measured in MD simulations as a function of ε_{appl} [Figs. 2 and 6(a)], G_K can be evaluated as a function of ε_{appl} [Fig. 6(b)] and v [Fig. 6(c)].

The radiated kinetic energy is carried by all traveling waves emitted from a moving dislocation. As long as the equipartition theorem holds for the radiated waves, the kinetic energy in Eq. (1) should be half of the total radiated

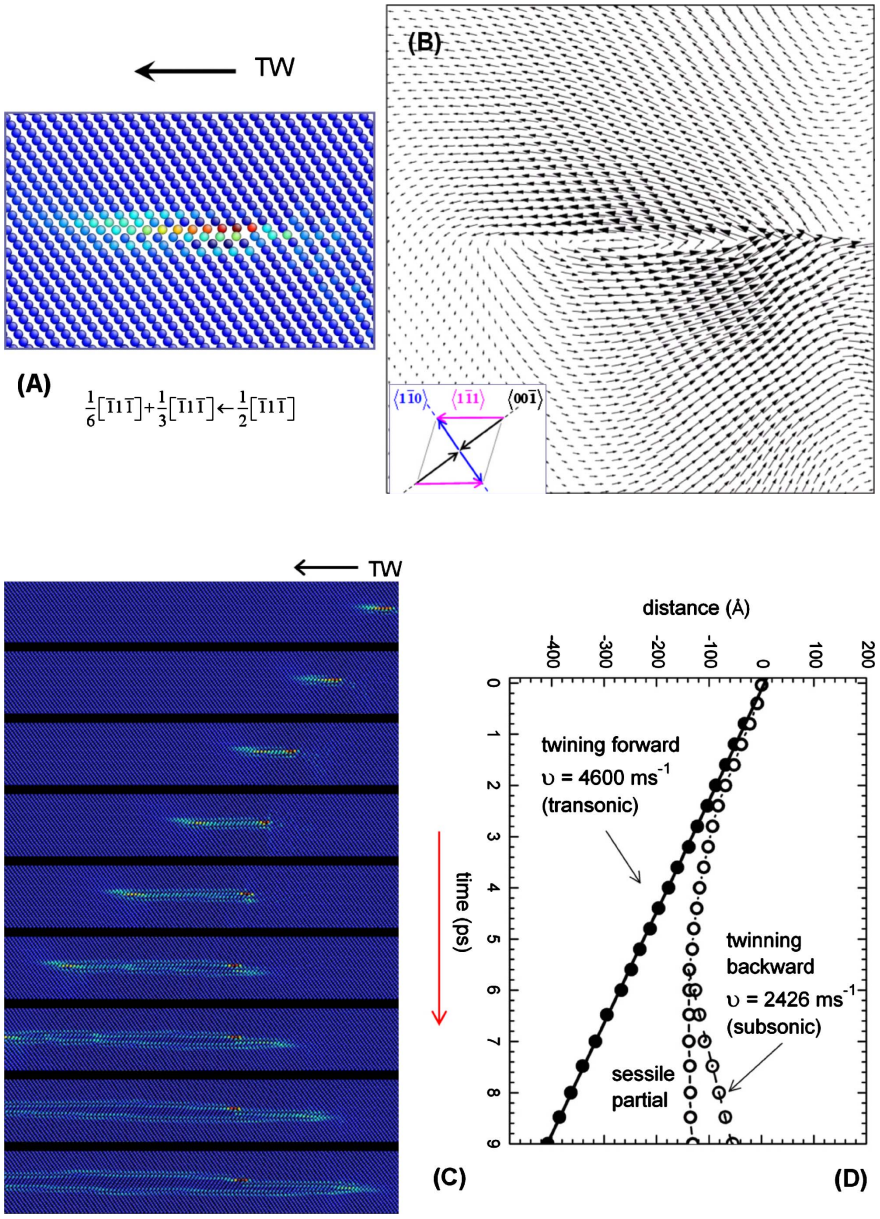

FIG. 5. (Color online) [(A) and (B)] Atomic profiles of a subsonic dislocation moving into the twinning direction ($v \sim 2400$ m s^{-1} at $\varepsilon_{appl}=-4\%$). Such a dislocation turned into an emissary dislocation, i.e., [(C) and (D)] it dissociates and triggers twinning.

energy (G_R) because an equal amount of the potential energy (or strain energy) should be carried by lattice waves.[41] Therefore, the total radiated energy should be twice that of G_K, i.e., $G_R \simeq 2G_K$.

The rate of energy radiation G_R plays the role of a drag force (radiation damping) on a moving dislocation. Since the motion is uniform, it must be counterbalanced by the driving force acting on the dislocation due to the applied shear strain, which is G_e given by Eq. (1). In our case, G_e measures the maximal elastic strain energy released by a moving dislocation. The force equilibrium condition for a uniform dislocation motion requires that

$$G_e = G_R \simeq 2G_K. \tag{5}$$

Such a force balance condition as a function of ε_{appl} can be checked straightforwardly by comparing $\frac{1}{2}G_e$ to G_K, as shown in Fig. 6(b). Both sets of data coincide and thus Eq. (5) is satisfied reasonably well which should hold for any uniform motion. It also provides a sanity check of nonlinear effects associated with adiabatic dislocation motion in our simulations.

In continuum elasticity theory,[12] it has been shown that for transonic and supersonic edge dislocations, the radiated energy (which is purely kinetic) can be calculated by extending Weertman's theoretical analysis[4] using a finite core width (w) within the Peierls-Nabarro dislocation model,

$$G_{th} = A(v)\frac{b^2}{2\pi w} = \frac{\mu}{2}R(v)\frac{b^2}{2\pi w}, \tag{6}$$

where

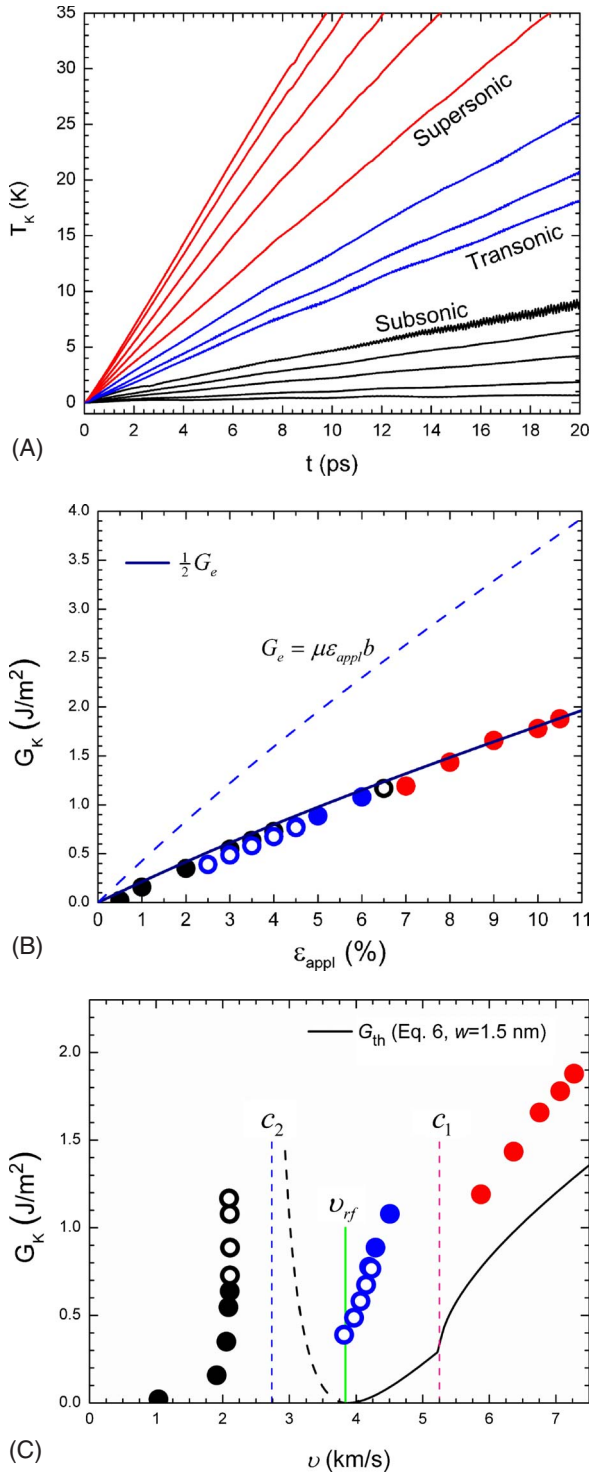

FIG. 6. (Color online) (A) System kinetic energy calculated as a function of time. Each curve corresponds to an independent simulation run where a different ε_{appl} has been applied to the standstill dislocation (from bottom, ε_{appl}=0.5%, 1%, 2%, 3%, 4%, 4.5%, 5%, 6%, 7%, 8%, 9%, 10%, and 10.5%, respectively). Within the time window the dislocation exhibits a uniform motion, G_K has been measured according to Eq. (4) and its ε_{appl} dependence is plotted in (B) in comparison with $G_e/2$ [see Eqs. (1) and (5)]. G_K versus dislocation velocity is shown in (C), where the theoretical solution based on Eq. (6) is obtained using $c_2=c_t(\varepsilon_0)$ and $c_1=c_l(\varepsilon_0)$ with ε_0=3%.

$$R(v)=\begin{cases}\dfrac{(\beta^2-1)\alpha^2}{\beta(1+\alpha^2)} & \text{for} \quad \sqrt{2}c_t<v<c_l \\ \dfrac{1}{\beta^2+1}\left[\dfrac{(\beta^2-1)^2}{\beta}+4\gamma\right] & \text{for} \quad v>c_l,\end{cases} \tag{7}$$

with $\alpha=\sqrt{(v^2/2c_t^2)-1}$, $\beta=\sqrt{(v^2/c_t^2)-1}$, and $\gamma=\sqrt{(v^2/c_l^2)-1}$. The v dependence of G_{th} has been plotted against our MD data in Fig. 6(c) where the core width of the dislocation is taken to be w=1.5 nm in accordance with the range of the observed value ($5\sim6b$) for transonic and/or supersonic dislocations in our MD simulations [see, e.g., Fig. 4(b)]. Evaluating the core width directly, we found that it decreases from the value of 1.5 nm by almost 20% as a subsonic dislocation approaches the Rayleigh wave velocity.

VI. DISCUSSION

The prediction of linear elasticity theory [Eq. (6)] is based on the elastic solution of moving dislocations with its stain and/or stress fields, self-energy, and effective mass as a function of v. Since the dynamical response of the dislocation core in a discrete and periodic lattice is not considered in the theory, the difference between MD computed radiation rate G_K and the theoretical prediction of Eq. (6) measures radiation due to the dislocation core in the discrete lattice. Most probably, a major contribution is associated with the excitation and scattering of lattice phonons at the highly strained, nonlinear, and anharmonic dislocation core regions.

For subsonic dislocations, the finite G_R due to core radiation results in a finite drag on dislocation motion which is very significant and easily overrules the well established inertial effects.[1] The drag significantly increases as the velocity approaches the Rayleigh wave speed. This is connected with a corresponding decrease in the core width of the dislocation. Such changes in the dislocation core effectively increase the barrier to transonic motion because the transition to transonic velocity with a wider core then requires not just the establishment of the appropriate radiation field but also a complete change in core structure.[5]

Such core contraction or distortion will eventually render the dislocation core mechanically unstable. Then, however, the outcome of the instability does not necessarily have to be a transonic dislocation. Core destabilization is related to different anomalous behavior[16,19,42] observed for "overloaded" fast moving subsonic dislocations such as microtwin nucleation.[18] This is in agreement with our results that a subsonic dislocation moving towards the twinning direction may dissociate and emit a microtwin (Fig. 5).

As discussed above, energy radiation in the continuum Peierls model [Eq. (6) and Fig. 6(c)] is incomplete due to the lack of consideration of phonon scattering and core radiation. Consequently, the radiation-free state at $v_{rf}=\sqrt{2}c_t$ is by no means radiation-free in real atomistic simulations. However, in agreement with Eq. (6), it is generally observed that a dislocation radiates more as it moves faster, $dG/dv>0$, which is true, in particular, at $v>v_{rf}$. This also agrees with the stable (steady-state) motion of dislocations in three dis-

tinct velocity regimes. In accordance with the continuum solution, a distinct drop in radiated energy is only observed for the transition from the subsonic to the transonic regime, while the transition from transonic to supersonic motion corresponds to a steady increase in radiation. In this second transition, elastic shear wave radiation into the shear wave Mach cone remains active but the shear wave radiation out of the dislocation core is apparently just left behind [Figs. 4(b) versus 4(c)] at the transition to supersonic motion.

The continuous behavior and the positive slop in the $v-\varepsilon_{appl}$ or the G_R-v plots [Figs. 2 and 4(b)] indicate that a transonic dislocation can be readily accelerated into the supersonic regime without being "overloaded." Consequently, the regimes of transonic and supersonic motion do not overlap in the $v-\varepsilon_{appl}$ diagram (Fig. 2), while there is an extended regime of loads in which subsonic and transonic or even supersonic dislocations can coexist.

Lattice wave emission from a radiating dislocation depends on the character of the dislocation. According to continuum theory,[4] a moving screw dislocation does not emit longitudinal waves and there exists no sound barrier between the subsonic motion ($v<c_t$) and supersonic motion ($v>c_t$) except for a single transonic state at $v=c_t$. In this case, it is expected that the core radiation plays a similar role as for edge dislocations, e.g., a subsonic screw dislocation cannot be accelerated to a supersonic state without jumping over a velocity gap, which is also found material dependent.[16] For dislocations of mixed character, the situation becomes more complex because the contributions to core radiation from the edge component and the screw component are strongly coupled. Similar to our current studies, quantitative analyses can in principle be carried out for screw or mixed dislocations based on available methods for nucleating transonic and/or supersonic dislocations.[5,43,44] On the other hand, our understanding of radiation mechanism in terms of lattice dynamics is still far from complete for both screw and nonscrew dislocations. To solve the problem, one needs to consider dispersion relations of lattice phonons.[6,14,15] In particular, as emitted from the dislocation core, the coupling between shear waves and longitudinal waves remains to be fully clarified for dislocation motions in different velocity regimes.

Our results (Figs. 2 and 3) indicate that the effect of anisotropy is not strong for highly loaded W. Simulations on tantalum and niobium, two bcc metals of different anisotropies, suggest that although waves can be emitted in quite different patterns, the physical picture of forces governing the dislocation motion is essentially the same as proposed here.

A critical question concerning the possibility to obtain transonic or supersonic dislocation motion in experiments was whether damping due to the scattering of lattice phonons at high temperatures would prevent the dislocations from reaching the transonic state. All previous simulations had been carried out at low temperatures where this damping is expected to be very small (e.g., Refs. 5, 12, and 14). Our simulation results presented here clearly demonstrate that the phonon damping cannot prevent dislocations from reaching the transonic velocity regime, although it appears that somewhat higher driving forces and/or loading rates are required to trigger and sustain transonic and supersonic motion at high temperatures as compared with low temperature cases.

VII. SUMMARY

We have performed atomistic simulations of fast moving edge dislocations in tungsten to clarify energy radiation at near-sonic, transonic, and supersonic velocities within a nearly isotropic lattice. Since force equilibrium has to be established between the driving force acting on the dislocation and the dragging force due to wave emissions, it could be demonstrated that the amount of energy radiated away from the dislocation can be measured from the kinetic energy in the system but can also be determined directly from the applied strain. In combination with elasticity analyses, it has been shown that lattice wave emission from the dislocation core plays an essential role for the achievable dislocation speed. Significant increases in radiation close to the Rayleigh wave velocity and in the transonic regime should make it difficult to reach transonic dislocation motion in real systems. However, it could clearly be demonstrated that phonon drag at higher temperatures does not prevent the dislocations from reaching transonic velocities.

ACKNOWLEDGMENTS

This research was supported by the Deutsche Forschungsgemeinschaft (DFG) under Contract No. Gu367-13. Part of the computation was performed at Max-Planck-Institut für Metallforschung. The authors thank D. M. Barnett and J. A. Zimmerman for kindly providing their anisotropy solutions for transonic and/or supersonic dislocation motions. Z.H. acknowledges discussions with E. Bitzek on atomistic simulations.

*jinzh@sjtu.edu.cn

[1] J. P. Hirth and J. Lothe, *Theory of Dislocations* (Wiley, New York, 1982).
[2] J. D. Eshelby, Proc. Phys. Soc., London, Sect. A **62**, 307 (1949).
[3] F. C. Frank, Proc. Phys. Soc., London, Sect. A **62**, 131 (1949).
[4] J. Weertman and J. R. Weertman, in *Dislocations in Solids*, edited by F. R. N. Nabarro (North-Holland, Amsterdam, 1980), Vol. 3, pp. 1–60.
[5] P. Gumbsch and H. Gao, Science **283**, 965 (1999).
[6] V. Celli and N. Flytzanis, J. Appl. Phys. **41**, 4443 (1970); S. Ishioka, J. Phys. Soc. Jpn. **30**, 323 (1971).
[7] V. L. Indenbom and J. Lothe, *Elastic Strain Fields and Dislocation Mobility* (North-Holland, Amsterdam, 1992).
[8] V. I. Alshits and V. L. Indenbom, in *Dislocations in Solids*, edited by F. R. N. Nabarro (North-Holland, Amsterdam, 1986), Vol. 7, Chap. 34.

[9] W. Cai, V. V. Bulatov, J. Chang, J. Li, and S. Yip, in *Dislocations in Solids*, edited by F. R. N. Nabarro and J. P. Hirth (North-Holland, Amsterdam, 1986), Vol. 12, Chap. 64.
[10] J. J. Gilman, Philos. Mag. A **76**, 329 (1997); Metall. Mater. Trans. A **31**, 811 (2000).
[11] J. P. Hirth, H. M. Zbib, and J. Lothe, Modell. Simul. Mater. Sci. Eng. **6**, 165 (1998).
[12] P. Gumbsch and H. Gao, J. Comput.-Aided Mater. Des. **6**, 137 (1999).
[13] E. Bitzek and P. Gumbsch, Mater. Sci. Eng., A **387-389**, 11 (2004).
[14] H. Koizumi, H. O. K. Kirchner, and T. Suzuki, Phys. Rev. B **65**, 214104 (2002).
[15] H. Koizumi and T. Suzuki, Mater. Sci. Eng., A **400-401**, 76 (2005).
[16] D. L. Olmsted, L. G. Hector, Jr., W. A. Curtin, and R. J. Clifton, Modell. Simul. Mater. Sci. Eng. **13**, 371 (2005).
[17] J. Marian, W. Cai, and V. V. Bulatov, Nat. Mater. **3**, 158 (2004).
[18] J. A. Young Vandersall and B. D. Wirth, Philos. Mag. **84**, 3755 (2004).
[19] S. Q. Shi, H. C. Huang, and C. H. Woo, Comput. Mater. Sci. **23**, 95 (2002).
[20] H. Gao, Y. Huang, P. Gumbsch, and A. J. Rosakis, J. Mech. Phys. Solids **47**, 1941 (1999).
[21] P. Rosakis, Phys. Rev. Lett. **86**, 95 (2001).
[22] F. F. Abraham and H. J. Gao, Phys. Rev. Lett. **84**, 3113 (2000).
[23] A. J. Rosakis, O. Samudrala, and D. Coker, Science **284**, 1337 (1999).
[24] K. Xia, A. J. Rosakis, and H. Kanamori, Science **303**, 1859 (2004).
[25] M. J. Buehler, F. F. Abraham, and H. J. Gao, Nature (London) **426**, 141 (2003).
[26] P. Rosakis and H. Tsai, Int. J. Solids Struct. **32**, 2711 (1995).
[27] J. Červ, M. Landa, and A. Machova, Scr. Mater. **43**, 423 (2000).
[28] J. Bosansky and T. Smida, Mater. Sci. Eng., A **323**, 198 (2002).
[29] K. Kadau, T. C. Germann, P. S. Lomdahl, and B. L. Holian, Science **296**, 1681 (2002).
[30] V. Nosenko, J. Goree, Z. W. Ma, D. H. E. Dubin, and A. Piel, Phys. Rev. E **68**, 056409 (2003).
[31] A. Sagy, Z. Reches, and J. Fineberg, Nature (London) **418**, 310 (2002).
[32] E. Olson and R. M. Allen, Nature (London) **438**, 212 (2005).
[33] V. Nosenko, S. Zhdanov, and G. Morfill, Phys. Rev. Lett. **99**, 025002 (2007).
[34] M. W. Finnis and J. E. Sinclair, Philos. Mag. A **50**, 45 (1984)5.
[35] G. J. Ackland and R. Thetford, Philos. Mag. A **56**, 15 (1987).
[36] A. T. Paxton, P. Gumbsch, and M. A. Methfessel, Philos. Mag. Lett. **63**, 267 (1991).
[37] DFT calculations of more realistic theoretical strength are available for W, see, e.g., D. Roundy, C. R. Krenn, M. L. Cohen, and J. W. Morris, Jr., Philos. Mag. A **81**, 1725 (2001).
[38] The atomic displacements and accompanying deformation of bonds across the slip plane lead to the presence of a periodic potential for dislocation motion. The concept of uniform motion is meaningful only when the observation time is sufficiently long such that the motion of dislocation over those energy barriers (the origin of wave emissions) can be considered as uniform.
[39] D. M. Barnett and J. A. Zimmerman, Nonradiating dislocations in uniform supersonic motion in anisotropic linear elastic solids, in *Integral Methods in Science and Engineering*, edited by P. Schiavone, C. Constanda, and A. Mioduchowski p. 45, (Birkhaeser, Boston, 2002); J. A. Zimmerman (private communications).
[40] A. W. Sleeswyk, Acta Metall. **10**, 705 (1962).
[41] I. G. Main, *Vibrations and Waves in Physics*, 2nd ed. (Cambridge University Press, Cambridge, 1984).
[42] J. Schiotz, K. W. Jacobsen, and O. H. Nielsen, Philos. Mag. Lett. **72**, 245 (1995).
[43] Z. H. Jin, P. Gumbsch, E. Ma, K. Albe, H. Hahn, and H. Gleiter, Scr. Mater. **54**, 1163 (2006).
[44] Z. H. Jin, P. Gumbsch, E. Ma, K. Albe, H. Gleiter, and H. Hahn, Acta Mater. **56**, 1126 (2008).